INTEGRATED BRAKING AND STEERING MODEL PREDICTIVE CONTROL APPROACH IN AUTONOMOUS VEHICLES

Paolo Falcone, Francesco Borrelli [*,1]
H. Eric Tseng, Jahan Asgari, Davor Hrovat [**]

[*] *Dipartimento di Ingegneria, Università del Sannio, 82100 Benevento, Italy*
{falcone,francesco.borrelli}@unisannio.it
[**] *Ford Research Laboratories, Dearborn, MI 48124, USA*
{htseng,jasgari,dhrovat}@ford.com

Abstract: In this paper we present a Model Predictive Control (MPC) approach for combined braking and steering systems in autonomous vehicles. We start from the result presented in (Borrelli et al. (2005)) and (Falcone et al. (2007a)), where a Model Predictive Controller (MPC) for autonomous steering systems has been presented. As in (Borrelli et al. (2005)) and (Falcone et al. (2007a)) we formulate an MPC control problem in order to stabilize a vehicle along a desired path. In the present paper, the control objective is to best follow a given path by controlling the front steering angle and the brakes at the four wheels independently, while fulfilling various physical and design constraints.

Keywords: Nonlinear Model Predictive Control, Active Steering, Autonomous Systems

1. INTRODUCTION

Recent trends in automotive industry point in the direction of increased content of electronics, computers, and controls with emphasis on the improved functionality and overall system robustness. Many advanced sensors and infrastructures and their vehicle active safety applications have been discussed in authors' previous publication (Falcone et al. (2007a)). Anticipating sensor and infrastructure trends toward increased integration of information and control actuation agents, we assume the ultimate information for obstacle avoidance will be available sometime in the future and we propose a double lane change scenario on a slippery road, with a vehicle equipped with fully autonomous steering and braking system.

It is therefore appropriate to ask how to best control the vehicle in following a desired obstacle avoidance trajectory as close as possible while maintaining vehicle speed and stability. The control inputs are the front steering and the braking at each of the four wheels. The measurements available to the controller through sensor fusion are the desired path, vehicle position, vehicle velocities and accelerations, yaw rate, as well as vehicle orientation information.

This will be done in the spirit of Model Predictive Control, MPC (Garcia et al. (1989); Mayne et al. (2000)) along the lines of our ongoing internal research efforts dating from early 2000 (Asgari and Hrovat (2002)).

[1] Corresponding author.

We use a model of the plant to *predict* the future evolution of the system (Mayne et al. (2000); Borrelli (2003); Keviczky et al. (2006)). Based on this prediction, at each time step t a performance index is optimized under operating constraints with respect to a sequence of future steering and braking moves in order to best follow the given trajectory on a slippery road. The first of such optimal moves is the *control* action applied to the plant at time t. At time $t+1$, a new optimization is solved over a shifted prediction horizon.

In (Borrelli et al. (2005)) a *nonlinear vehicle model* is considered to *predict* the future evolution of the system (Mayne et al. (2000)). The resulting MPC controller requires a non-linear optimization problem to be solved at each time step. Although good results have been achieved, even at high vehicle speed, the computational burden is a serious obstacle for experimental validation. In (Falcone et al. (2007a)) a sub-optimal MPC steering controller based on successive on-line linearizations of the non-linear vehicle model is presented. The method stems from an accurate analysis of the vehicle nonlinearities, the constraints and the performance index in the optimal control problem. The presented experimental results demonstrated that the controller can stabilize the vehicle even at high speed on slippery surfaces.

In this paper we reformulate the path following control problem in (Borrelli et al. (2005)) and (Falcone et al. (2007a)), as a MPC control problem where the control inputs are the front steering angle and the braking torque at the four wheels. The MPC formulation relies on a full four wheels nonlinear model including the tire nonlinearities.

The paper is structured as follows. Section 2 describes the vehicle dynamical model used with a brief discussion on tire models. Section 3 formulates the control problem. The considered scenario is presented in Section 4. Simulation and experimental results will be presented in the final version of the paper, if accepted.

2. MODELING

This section describes the vehicle and tire model we used for simulations and control design. The nomenclature refers to the model depicted in Figure 1. We denote by F_l, F_c the longitudinal (or "tractive") and lateral (or "cornering") tire forces, respectively, F_x, F_y the longitudinal and lateral forces acting on the vehicle center of gravity, F_z the normal tire load, X, Y the absolute car position inertial coordinates, a, b (distance of front and rear wheels from center of gravity) and c (distance of the vehicle longitudinal axis from the wheels) the car geometry, g the gravitational constant, m the car mass, I the car inertia, I_d the driveline inertia, B_d the damping coefficient of the driveline, r the wheel radius, s the slip ratio, μ the road friction coefficient, v_l, v_c the longitudinal and lateral wheel velocities and v_x, v_y their resultants along the longitudinal and lateral vehicle axes respectively, ψ the heading angle, $\dot{x}$ and $\dot{y}$ the vehicle longitudinal and lateral speed respectively, α the tire slip angle, δ the wheel steering angle, T_b the brake torque at the brake pad. The lower scripts $(\cdot)_f$ and $(\cdot)_r$ particularize a variable at the front wheels and the rear wheels, respectively, e.g. F_{l_f} is the front wheel longitudinal force.

2.1 Vehicle Model

We use a four wheels model to describe the dynamics of the car and assume constant normal tire load, i.e., $F_{z_{f,l}}, F_{z_{f,r}}, F_{z_{r,l}}, F_{z_{r,r}} = \text{constant}$. Such model captures the most relevant nonlinearities associated to lateral stabilization of the vehicle. Figure 1 depicts a diagram of the vehicle model, which has the following longitudinal, lateral and turning or yaw degrees of freedom (DOF)

$$m\ddot{x} = m\dot{y}\dot{\psi} + F_{x_{f,l}} + F_{x_{f,r}} + F_{x_{r,l}} + F_{x_{r,r}}, \quad (1a)$$

$$m\ddot{y} = -m\dot{x}\dot{\psi} + F_{y_{f,l}} + F_{y_{f,r}} + F_{y_{r,l}} + F_{y_{r,r}}, \quad (1b)$$

$$I\ddot{\psi} = a\left(F_{y_{f,l}} + F_{y_{f,r}}\right) - b\left(F_{y_{r,l}} + F_{y_{r,r}}\right) \quad (1c)$$

$$+ c\left(-F_{x_{f,l}} + F_{x_{f,r}} - F_{x_{r,l}} + F_{x_{r,r}}\right). \quad (1d)$$

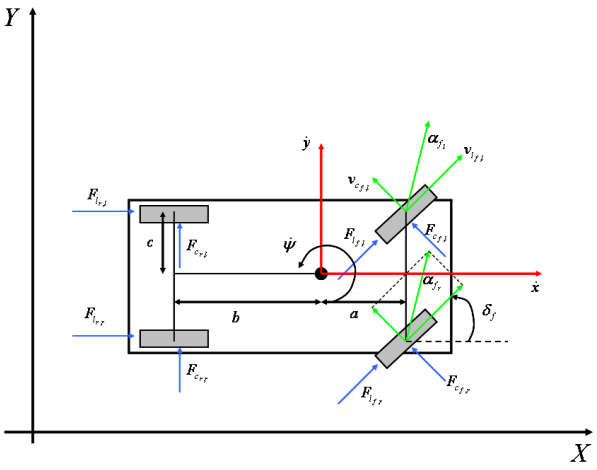

Fig. 1. The simplified vehicle dynamical model.

The vehicle's equations of motion in an absolute inertial frame are

$$\dot{Y} = \dot{x}\sin\psi + \dot{y}\cos\psi, \quad (2a)$$

$$\dot{X} = \dot{x}\cos\psi - \dot{y}\sin\psi. \quad (2b)$$

The longitudinal and lateral forces generated by the four tires lead to the following forces acting on the center of gravity:

$$F_y = F_l \sin\delta + F_c \cos\delta, \tag{3a}$$
$$F_x = F_l \cos\delta - F_c \sin\delta. \tag{3b}$$

Tire forces for each tire are given by

$$F_l = f_l(\alpha, s, \mu, F_z), \tag{4a}$$
$$F_c = f_c(\alpha, s, \mu, F_z), \tag{4b}$$

where α is the slip angle of the tire, s is the slip ratio defined as

$$s = \begin{cases} s = \dfrac{r\omega}{v_l} - 1 \text{ if } v_l > r\omega, v \neq 0 \text{ for braking} \\ s = 1 - \dfrac{v_l}{r\omega} \text{ if } v_l < r\omega, \omega \neq 0 \text{ for driving} \end{cases} \tag{5}$$

where v_l is the longitudinal wheel velocity, r and ω are the wheel radius and angular speed respectively. By assuming that the vehicle is traveling at zero engine torque, the wheels angular speeds are obtained, for the four wheels, by integrating the following set of differential equations

$$I_{d,f}\dot{\omega}_{fl} = -F_{l_{f,l}} r - T_{b_{f,l}} - B_d \omega_{f,l}, \tag{6a}$$
$$I_{d,f}\dot{\omega}_{fr} = -F_{l_{f,r}} r - T_{b_{f,r}} - B_d \omega_{f,r}, \tag{6b}$$
$$I_{d,r}\dot{\omega}_{rl} = -F_{l_{r,l}} r - T_{b_{r,l}} - B_d \omega_{r,l}, \tag{6c}$$
$$I_{d,r}\dot{\omega}_{rr} = -F_{l_{r,r}} r - T_{b_{r,r}} - B_d \omega_{r,r}. \tag{6d}$$

The slip angle represents the angle between the wheel velocity and the direction of the wheel itself:

$$\alpha = \tan^{-1} \frac{v_c}{v_l}. \tag{7}$$

In equations (5) and (7), v_c and v_l are the lateral (or cornering) and longitudinal wheel velocities, respectively, which are expressed as

$$v_l = v_y \sin\delta + v_x \cos\delta, \tag{8a}$$
$$v_c = v_y \cos\delta - v_x \sin\delta, \tag{8b}$$

and

$$v_{y_{f,l}} = \dot{y} + a\dot{\psi} \quad v_{x_{f,l}} = \dot{x} - c\dot{\psi}, \tag{9a}$$
$$v_{y_{f,r}} = \dot{y} + a\dot{\psi} \quad v_{x_{f,r}} = \dot{x} + c\dot{\psi}, \tag{9b}$$
$$v_{y_{r,l}} = \dot{y} - b\dot{\psi} \quad v_{x_{r,l}} = \dot{x} - c\dot{\psi}, \tag{9c}$$
$$v_{y_{r,r}} = \dot{y} - b\dot{\psi} \quad v_{x_{r,r}} = \dot{x} + c\dot{\psi}. \tag{9d}$$

The parameter μ in (4) represents the road friction coefficient and F_z is the total vertical load of the vehicle. This is distributed between the front and rear wheels based on the geometry of the car model, described by the parameters a and b:

$$F_{z_f} = \frac{bmg}{2(a+b)}, \quad F_{z_r} = \frac{amg}{2(a+b)}. \tag{10a}$$

Using the equations (1)-(10), the nonlinear vehicle dynamics can be described by the following compact differential equation assuming a certain friction coefficient value μ:

$$\dot{\xi} = f_\mu(\xi, u), \tag{11a}$$
$$\eta = h(\xi), \tag{11b}$$

where the state and input vectors are $\xi = [\dot{y},\ \dot{x},\ \psi,\ \dot{\psi},\ Y,\ X,\ \omega_{f,l},\ \omega_{f,r},\ \omega_{r,l},\ \omega_{r,r}]$ and

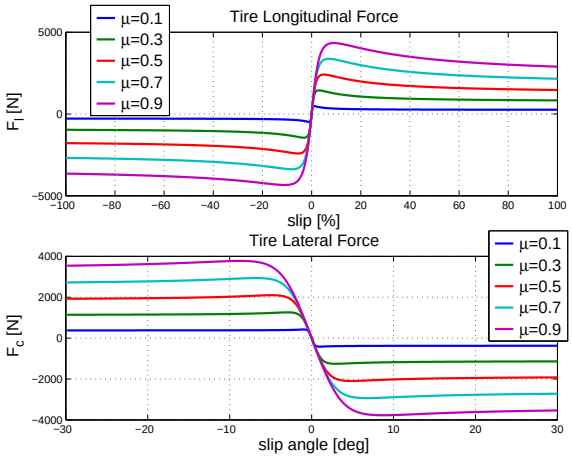

Fig. 2. Longitudinal force in pure braking/driving (upper plot) and ateral force in pure cornering (lower plot).

$u = [\delta_f,\ T_{b_{f,l}},\ T_{b_{f,r}},\ T_{b_{r,l}},\ T_{b_{r,r}}]$ respectively, and the output map is given as

$$h(\xi) = \begin{bmatrix} 0&1&0&0&0&0&0&0&0&0 \\ 0&0&1&0&0&0&0&0&0&0 \\ 0&0&0&1&0&0&0&0&0&0 \\ 0&0&0&0&1&0&0&0&0&0 \end{bmatrix} \xi. \tag{12}$$

2.2 Tire Model

The model for tire tractive and cornering forces (4) used in this paper is described by a Pacejka model (Bakker et al. (1987)). This is a complex, semi-empirical model that takes into consideration the interaction between the tractive force and the cornering force in combined braking and steering. The longitudinal and cornering forces are assumed to depend on the normal force, slip angle, surface friction, and longitudinal slip. Sample plots of predicted longitudinal and lateral force versus longitudinal slip and slip angle are shown in Figure 2. These plots are shown for a single tire.

3. MODEL PREDICTIVE CONTROL PROBLEM

We design a MPC controller computing the front steering angle and the braking torques at the four wheels, such that the a desired path is followed as close as possible at a given longitudinal speed.

In order to obtain a finite dimensional optimal control problem we consider the model (11) and discretize the system dynamics with the Euler method, to obtain

$$\xi(k+1) = f_\mu^{dt}(\xi(k), u(k)), \tag{13a}$$
$$u(k) = u(k-1) + \Delta u(k), \tag{13b}$$
$$\eta(k) = h(\xi(k)), \tag{13c}$$

where $u(k) = [\delta_f,\ T_{b_{f,l}},\ T_{b_{f,r}},\ T_{b_{r,l}},\ T_{b_{r,r}}]$, $\Delta u(k) = [\Delta\delta_f(k), \Delta\, T_{b_{f,l}}, \Delta\, T_{b_{f,r}}, \Delta\, T_{b_{r,l}},\ \Delta\, T_{b_{r,r}}]$.

We consider the following cost function:

$$J(\xi(t), \Delta\mathcal{U}_t) = \sum_{i=1}^{H_p} \left\| \hat{\eta}_{t+i,t} - \eta_{ref_{t+i,t}} \right\|_Q^2 + \\ + \sum_{i=0}^{H_c-1} \|\Delta u_{t+i,t}\|_R^2 + \sum_{i=0}^{H_c-1} \|u_{t+i,t}\|_S^2 \tag{14}$$

where, as in standard MPC notation (Mayne et al. (2000)), $\Delta\mathcal{U}_t = [\Delta u_{t,t}, \ldots, \Delta u_{t+H_c-1,t}]$ is the optimization vector at time t and $\hat{\eta}_{t+i,t}$ denotes the output vector predicted at time $t+i$ obtained by starting from the state $\xi_{t,t} = \xi(t)$ and applying to system (13) the input sequence $\Delta u_{t,t}, \ldots, \Delta u_{t+i,t}$. H_p and H_c denote the output prediction horizon and the control horizon, respectively. As in standard MPC schemes, we use $H_p > H_c$ and the control signal is assumed constant for all $H_c \leq t \leq H_p$, i.e., $\Delta u_{t+i,t} = 0\ \forall i \geq H_c$. The reference signal η_{ref} represents the desired outputs, where $\eta = [\dot{x}, \psi, \dot{\psi}, Y]'$. Q, R and S are weighting matrices of appropriate dimensions. In (14) the first summand reflects the desired performance on target tracking, the second and the third summands are a measure of the steering and braking effort.

The minimization of (14) subject to the model equation (13) is the base of the NLMPC scheme presented in (Borrelli et al. (2005)).

In this article we consider the LTV-MPC scheme presented in (Falcone et al. (2007a,b)) based on the following optimization problem:

$$\min_{\Delta\mathcal{U}_t} \ J(\xi_t, \mathcal{U}_t) \tag{15a}$$

subj. to

$$\xi_{k+1,t} = \mathcal{A}_t \xi_{k,t} + \mathcal{B}_t u_{k,t} + d_{k,t}, \tag{15b}$$
$$k = t, \ldots, t+H_p-1$$

$$\begin{bmatrix} \alpha_{f_{k,t}} \\ \alpha_{r_{k,t}} \end{bmatrix} = \mathcal{C}_t \xi_{k,t} + \mathcal{D}_t u_{k,t} + e_{k,t} \tag{15c}$$

$$\eta_{k,t} = h\left(\xi_{k,t}\right), \tag{15d}$$
$$k = t+1, \ldots, t+H_p$$

$$u_{k,t} = u_{k-1,t} + \Delta u_{k,t}, \tag{15e}$$
$$k = t, \ldots, t+H_c-1$$

$$u_{t-1,t} = u(t-1) \tag{15f}$$

$$u_{f,min} \leq u_{k,t} \leq u_{f,max} \tag{15g}$$
$$k = t, \ldots, t+H_p-1$$

$$\Delta u_{f,min} \leq \Delta u_{k,t} \leq \Delta u_{f,max} \tag{15h}$$
$$k = t, \ldots, t+H_c-1$$

$$\alpha_{f_{min}} \leq \alpha_{f_{k,t}} \leq \alpha_{f_{max}} \tag{15i}$$

$$\alpha_{r_{min}} \leq \alpha_{r_{k,t}} \leq \alpha_{r_{max}} \tag{15j}$$
$$k = t+1, \ldots, t+H_p$$

where the equations (15b)-(15d) are a discrete linear approximation of (13) computed at the current state $\xi(t)$ and the previously applied control input $u(t-1)$. The terms $d_{k,t}$ and $e_{k,t}$, in (15b) and (15c) respectively, take into account that the operating point $\xi(t)$, $u(t-1)$ in general in not an equilibrium point. Further details can be found in (Falcone et al. (2007b)). The optimization problem (15) can be recast as a quadratic program (QP) (details can be found in (Borrelli et al. (2005))) and the resulting MPC controller for a Linear Time Varying (LTV) system will solve the problem (15) at each time step. Once a solution $\Delta\mathcal{U}_t^*$ to problem (15) has been obtained, the input command is computed as

$$u(k) = u(k-1) + \Delta u_{t,t}^*, \tag{16}$$

where $\Delta u_{t,t}^*$ is the vector of the first five elements of $\Delta\mathcal{U}_t^*$. At the next time step, the linear model (15b)-(15d) is computed based on new state and input measurements, and the new QP problem (15) is solved over a shifted horizon. In constraints (15i), (15j) the predictions $\alpha_{f_{k,t}}$ and $\alpha_{r_{k,t}}$ of the front and rear tire slip angles are computed according to the equations (7)-(9).

Complexity of (15) reduces compared to the NLMPC in (Borrelli et al. (2005)), and it is function of the time needed to setup the problem (15), i.e., to compute the linear models $(\mathcal{A}_t, \mathcal{B}_t, \mathcal{C}_t, \mathcal{D}_t)$ in (15b)-(15d) along the trajectory, and of the time to solve it.

As in (Falcone et al. (2007a)), the stability of the closed loop system is enforced through the *ad hoc* constraints (15i), (15j). In particular, without the constraints (15i), (15j) the performance of the linear MPC controller (15)-(16) is not acceptable and sometime unstable. This is due to the fact that a simple linear model is not able to predict the change of slope in the tires characteristic (see Figure (2)). To overcome this issue we add constraints (15i), (15j) to the optimization problem, in order to forbid the system from entering into a strongly nonlinear and possibly unstable region of the tire characteristic. In particular, by looking at the tire characteristic in the lower plot of Figure 2, it is clear that the tire slip angles α should be constrained in a range where the lateral forces are linear functions of the front slip angle. The same holds true for the longitudinal tire forces as function of the slip ratio. Note that the (15i), (15j) are implicit nonlinear constraints on state and input and they can be handled systematically only in a MPC scheme. A more general stability constraint has been proposed in (Falcone et al. (2007b)). In this paper, tire slip angle constraints are used to maintain vehicle stability.

4. RESULTS

We considered a scenario where the objective is to follow a desired path as close as possible on a snow covered road ($\mu = 0.3$) at a given desired speed. The control inputs in our scenario are the front tire steering angle and the brake torques at the four wheels and the goal is to follow the trajectory as close as possible by minimizing the vehicle deviation from the target path. The experiment is repeated with increasing entry speeds until the vehicle loses control. Figures 3-6 show the simulation and experimental results of the controller (15)-(16) with $\dot{x}_{ref} = 13.9$m/s (50 Kph) and the following tuning:

- *sample time*: $T = 0.05$ sec;
- *constraints on inputs and input rates*: $\delta_{f,min}$=-10 deg, $\delta_{f,max}$=10 deg, $\Delta\delta_{f,min}$=-0.85 deg, $\Delta\delta_{f,max}$=0.85 deg. The upper and lower bounds on the four brake torques are 0 and 600 Nm respectively (i.e. the vehicle can brake only), the bounds on the braking rate are $\pm$58.3 Nm per sampling time.
- *constraints on the tire slip angles*: $\alpha_{f_{min}} = -2.5$ deg, $\alpha_{f_{max}} = 2.5$ deg, $\alpha_{r_{min}} = -2.5$ deg, $\alpha_{r_{max}} = 2.5$ deg.
- *weights on tracking errors*: $Q_{\dot{x}} = 1$, $Q_{\psi} = 10$, $Q_{\dot{\psi}} = 1$, $Q_Y = 30$, $Q_{ij} = 0$ for $i \neq j$;
- *weights on input rates*: $R_{\delta_f} = 10$, $R_{T_{b_{f,l}}} = 10$, $R_{T_{b_{f,r}}} = 10$, $R_{T_{b_{r,l}}} = 10$, $R_{T_{b_{r,r}}} = 10$, $R_{ij} = 0$ for $i \neq j$;
- *weights on input*: $S_{i,j} = 10^{-1}$, for $i = j$, $S_{i,j} = 0$, for $i \neq j$;
- *horizons*: $H_p = 15$, $H_c = 2$.

The simulation results have been obtained in simulation with a 2.0 GHz Centrino-based laptop running Matlab 6.5. A description of the experimental setup can be found in (Falcone et al. (2007a)).

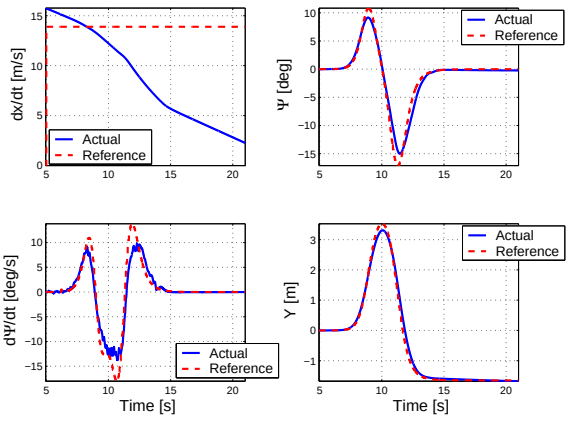

Fig. 3. Simulation results at 50 kph. Tracking variables.

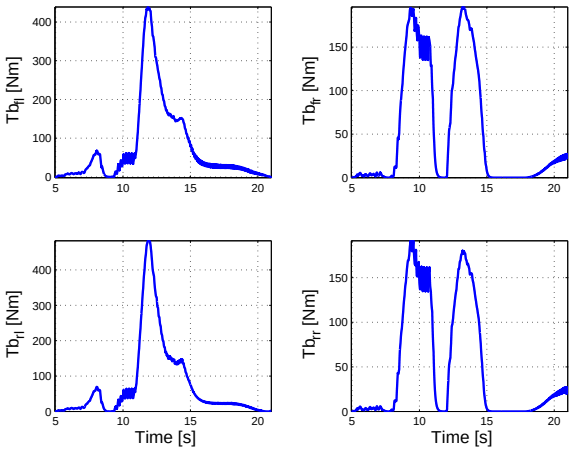

Fig. 4. Simulation results at 50 kph. Brake torques.

Figures 3 and 5 show the tracking variables in simulation and experiments respectively. In Figures 4 and 6 the corresponding brake torques are reported, while Figure 7 shows the steering angle in simulation (upper plot) and experiment (lower plot). In particular in Figure 6 we observe the desired brake torques computed by the controller (solid line) and the torques delivered by the braking system (dashed line). In the experiment an unavoidable steering disturbance (dash-dotted line) from the driver holding the steering wheel affects the actual steering angle (or "measured input" shown by dashed line).

By comparing the tracking variables in simulation and experiment we observe in both cases an overall good tracking of the desired path.

In the experimental results in Figure 5 we observe that an oscillation in the yaw rate occurs as the vehicle try to steer back to its original lane, around approximately 11 s. This is believed to be caused by excessive counter steering effort and stabilizing brake torque, followed by steering for path following recovery. The cause for the excessive steering/braking input is believed to be the result of model mismatch since the actual plant deviates from the predicted model (obtained by linearization at large slip angle) once the stabilizing steering/braking input is applied.

We demonstrated that the MPC steering and braking path following performance can be predicted in our simulations. As such, further tuning in the active steering and breaking distribution can be performed based on simulations to adjust the trade off between path following performance and exiting vehicle speed or braking intrusiveness.

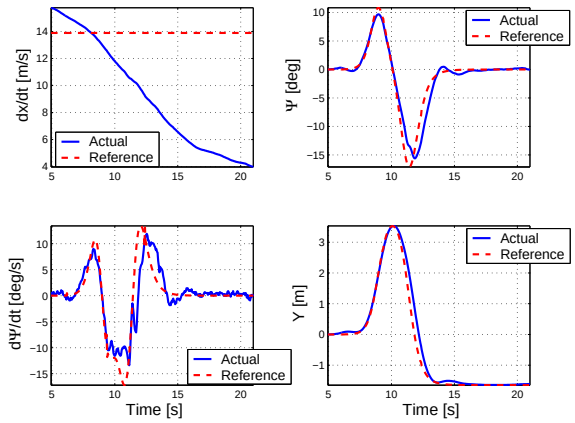

Fig. 5. Experimental results at 70 kph. Tracking variables.

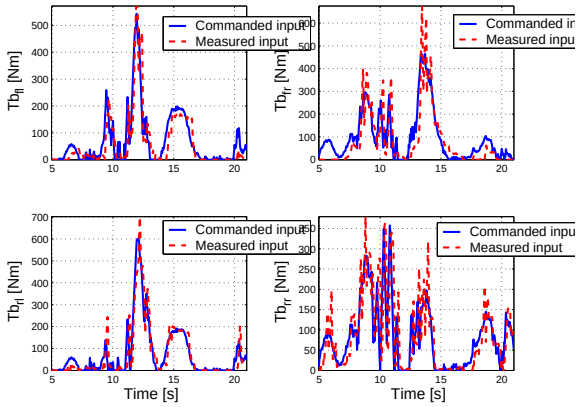

Fig. 6. Experimental results at 70 kph. Brake torques.

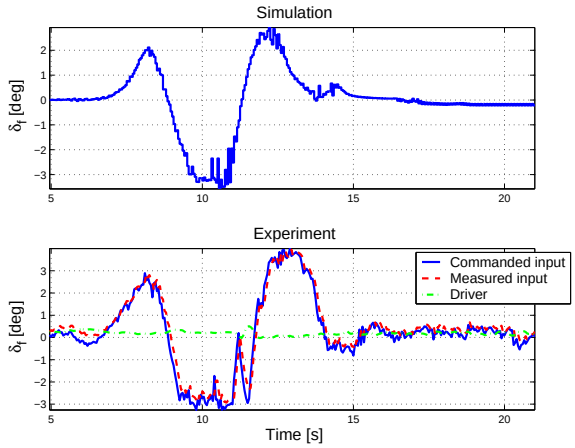

Fig. 7. Simulation results (upper plot) and experimental results (lower plot) at 50 kph. Steering angle.

5. CONCLUSIONS

We presented an integrated braking and steering Model Predictive Control for autonomous path following. The presented approach has been tested both in simulations and experiments with a double lane change manoeuvre on a snow covered road at high speed. The results showed an overall good tracking of the desired path. This is also due to the capability of slowing down the vehicle thanks to the braking. Future activities will aim to integrate further control inputs, like the engine torque and active differential, in order to well track the longitudinal velocity reference as well.

REFERENCES

J. Asgari and D. Hrovat. *Potential benefits of Interactive Vehicle Control Systems*. Ford Motor Company, Dearborn (USA). Internal Report, 2002.

E. Bakker, L. Nyborg, and H. B. Pacejka. Tyre modeling for use in vehicle dynamics studies. *SAE paper # 870421*, 1987.

F. Borrelli. *Constrained Optimal Control of Linear and Hybrid Systems*, volume 290 of *Lecture Notes in Control and Information Sciences*. Springer, 2003.

F. Borrelli, P. Falcone, T. Keviczky, J. Asgari, and D. Hrovat. MPC-based approach to active steering for autonomous vehicle systems. *Int. J. Vehicle Autonomous Systems*, 3(2/3/4):265–291, 2005.

P. Falcone, F. Borrelli, J. Asgari, H. E. Tseng, and D. Hrovat. Predictive active steering control for autonomous vehicle systems. *To appear on IEEE Trans. on Control System Technology* (available at http://www.grace.ing.unisannio.it/publication/416), 2007a.

P. Falcone, F. Borrelli, J. Asgari, H. E. Tseng, and D. Hrovat. Linear time varying model predictive control and its application to active steering systems: Stability analisys and experimental validation. *Submitted to International Journal of Robust and Nonlinear Control* (available at http://www.grace.ing.unisannio.it/publication/414), 2007b.

C.E. Garcia, D.M. Prett, and M. Morari. Model predictive control: Theory and practice-a survey. *Automatica*, 25:335–348, 1989.

T. Keviczky, P. Falcone, F. Borrelli, J. Asgari, and D. Hrovat. Predictive control approach to autonomous vehicle steering. In *Proc. American Contr. Conf.*, Minneapolis, Minnesota, 2006.

D.Q. Mayne, J.B. Rawlings, C.V. Rao, and P.O.M. Scokaert. Constrained model predictive control: Stability and optimality. *Automatica*, 36(6):789–814, June 2000.